

# Numerical Analysis of Distance Effect between Inducer and Centrifugal Impeller in Independent Rotational Turbopump in Co-rotating and Counter-rotating Mode

**E. DEHNAVI<sup>a</sup>, F. BAKIR<sup>b</sup>, A. DANLOS<sup>b</sup>, M. KEBDANI<sup>b</sup>**

- a. Arts et Métiers Institute of Technology, LIFSE, Le Cnam, HESAM University, 75013 Paris, France, [ehsan.dehnavi@ensam.eu](mailto:ehsan.dehnavi@ensam.eu)
- b. Arts et Métiers Institute of Technology, LIFSE, Le Cnam, HESAM University, 75013 Paris, France

## **Abstract:**

This study focuses on enhancing the performance of turbomachines through the design of multi-rotor configurations. Specifically, the effect of the distance between an axial inducer and a centrifugal impeller, which rotates independently in both co-rotation and counter-rotation modes, is investigated in a turbopump. The study parameters include the speed ratio and the distance between the inducer and impeller. Numerical results for the centrifugal impeller are validated through experimental testing, and two inducers with the same geometrical characteristics but with inverse tip angles are designed. Results show that changing the distance between the inducer and impeller, as well as the speed ratio, can have a significant impact on the turbomachine's performance.

**Keywords:** Turbopump, Counter rotative pump, Co-rotative pump, Inducer, Centrifugal impeller, Cavitation

## Introduction

Centrifugal pumps are an essential component of the oil and petroleum industries due to their flexible design and compact construction [1]. In pumps, an axial impeller called the inducer is placed in front of the primary centrifugal impeller to increase the Net Positive Suction Head Required (NPSHr), which prevents performance loss by raising the impeller's inlet pressure and develops performance at the nominal point. Centrifugal impellers with inducers are used in numerous industries, including the nuclear industry, aircraft, marine industry, and pumping of cryogenic propellants.

Coutier-Delgosha et al. [3] conducted a numerical investigation of the cavitation behavior of the inducer. The study by Guo et al. [4] showed that the number of inducer blades has a significant effect on both the head and the anti-cavitating performance of the pump. Their study on the effect of rotational speed on the performance of the pumps also demonstrated that increasing the rotational speed of the pump decreased its anti-cavitating performance [5]. Magne et al. [6] experimentally investigated the impact of dissolved CO<sub>2</sub> and jet fuel on the performance of a three-bladed inducer, revealing that, while the concentration of CO<sub>2</sub> has little effect on inducer efficiency for any rotational speed under non-cavitation conditions, it has a significant effect under cavitation conditions.

Xu et al. [7] conducted a visual experimental study of a high-speed inducer, revealing the development of a vortex at the inducer's inlet that rotates approximately at half the speed of the inducer. In addition, as the flow rate increases, the volume of the backflow vortex diminishes until it completely disappears at a flow rate higher than 30% of the design flow rate. Campos-Amezcuca et al. [8] studied the cavitating flow through an axial two-bladed inducer considering tip clearance. According to the performance analysis of a centrifugal pump with variable pitch inducers rotating at various speeds [9], the number of static head rises as rotation speed increases. However, when the rotation speed increases, the NPSHr grows, indicating a higher risk of cavitation in the pump. Kim et al. [10] investigated the impact of existing inducers on centrifugal impellers, showing that, under non-cavitating conditions, inducers increase head and efficiency at low flow rates while decreasing both at high flow rates.

In recent decades, the need for more efficient and reliable turbomachines has driven scientists and industries to move away from conventional single-blade propellers and design counter-rotating turbomachines. This article discusses the numerical analysis of independently rotating inducers and centrifugal impellers at various distances. This allows the inducer to rotate independently thanks to a novel geometry that has been designed for the pump. Additionally, two inducers that have the same geometry, but a reverse angle of attack have been developed so that they can rotate in co-rotation and counter-rotation modes to analyze the impact of the rotation direction on the pump's characteristics.

## Numerical method and geometry

This article presents a study on a pump consisting of a centrifugal impeller and an inducer. The centrifugal impeller with six blades, an inner diameter of 79 mm, and a tip diameter of 134 mm was selected for this analysis. A three-bladed inducer with a 24 mm inner diameter and a 78 mm (Dio) tip diameter was mounted 2 mm upstream of the centrifugal impeller at the first step. The tip clearance of the inducer was 1 mm.

To perform the computational fluid dynamics (CFD) simulation, StarCCM+ 16.06 software was used, applying the  $k-\epsilon$  standard model as the turbulence model to resolve the steady-state Reynolds-averaged Navier-Stokes (RANS) equations. To achieve maximum accuracy for the new independent rotating configuration, it was necessary to simulate the complete geometry. Figure 1 shows the different parts of the geometry with the applied mesh. The simulated geometry was divided into several parts, including an inlet, co-rotative and counter-rotative inducers, centrifugal impeller, diffuser, and outlet. The two parts of the inducer and the impeller were defined as rotating parts, and according to the new system of independent rotation, each rotor was defined as a separate rotating part. This enabled different rotational speeds to be applied, as well as the ability to change the direction of rotation of the inducers. Although the simulated geometry was more complicated and resulted in higher simulation time and cost, it was necessary to obtain accurate results.

During the simulation, a three-dimensional steady-state flow with constant density was considered as the flow model.

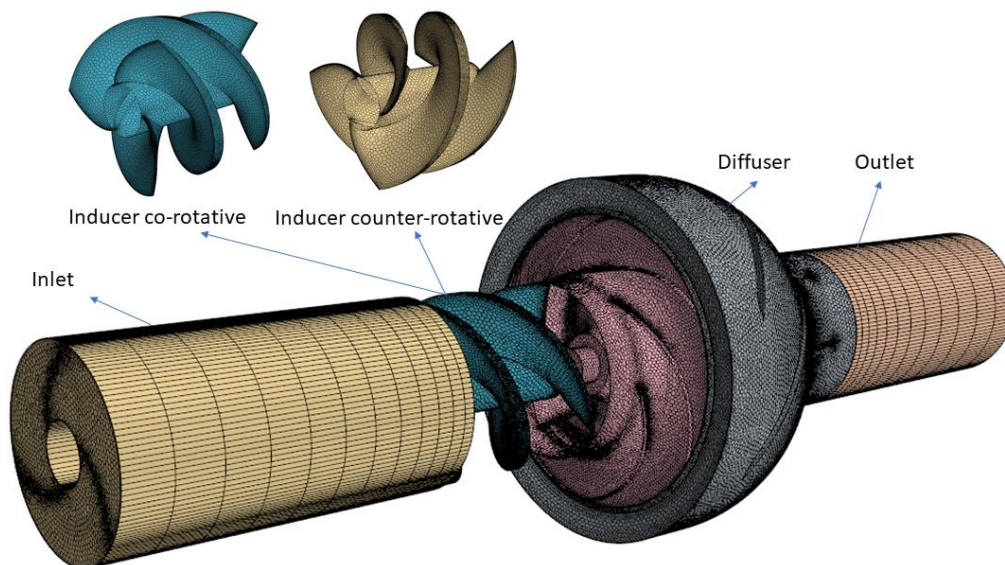


Figure 1 Schematic of pump for co-rotating and counter-rotating inducer with simulation meshing parts

## Mesh independency

Choosing the appropriate mesh is a critical part of any simulation, as the computational cost can be high. The mesh must be accurate enough to satisfy simulation requirements without adding to the computing time or cost. Checking mesh independence is crucial to achieving this goal in two ways. First, it ensures that the mesh has a sufficient number of cells to provide accurate results without incurring high computational costs. In this study, the sensitivity of

efficiency to seven different meshes was analyzed to determine the optimal number of meshes. A polyhedral mesh was used in the domain, with surface controls and prism layers to increase simulation accuracy. An unstructured mesh with a base size of 20mm was used for the inducer, impeller, and diffuser, while 4 and 6 prism layers with 2% of mesh base size were applied in the inducer and impeller parts, respectively.

Mesh independence was studied for the Design Operating Point (DOP) for SR=1. Figure 2 shows that the efficiency, as a study parameter, converged at mesh number 5. Increasing the mesh number did not significantly affect the results but only increased computational time and cost. Therefore, it can be concluded that mesh number 5 is the optimal number of cells.

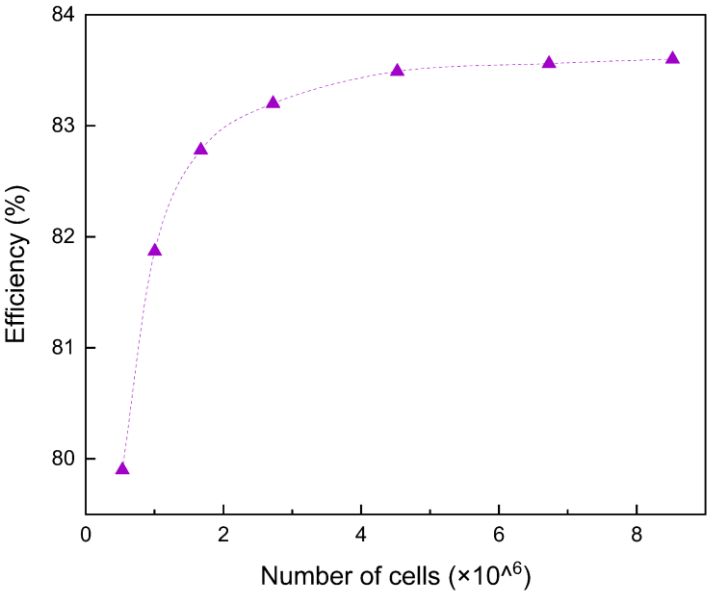


Figure 2 Efficiency comparison with different mesh cells

Table 1 describes the number of cells that were used in different parts of the geometry. The total number of cells for the complete configuration was 4,523,959, as shown in Table 1, along with the number of meshes applied to each part.

Table 1 Applied mesh on different parts

	Mesh 1	Mesh 2	Mesh 3	Mesh 4	Mesh 5	Mesh 6	Mesh 7
Inlet	16044	30720	47580	59592	59400	74892	103776
Inducer	9802	175136	352892	572586	1110290	1876380	2169832
Impeller	112471	235946	463991	829227	1644861	2355385	2682727
Diffuser	293592	545859	791558	1229511	1679312	2367817	3476223
Outlet	12564	16692	16824	30096	30096	53040	89700
Total	532698	1004353	1672845	2721012	4523959	6727514	8522258

## Experimental validation

Experimental tests were conducted at a rotational speed of 1480 rpm on the same pump geometry without an inducer. To compare the results with the experimental testing and validate the numerical model, the centrifugal impeller was simulated without an inducer at a speed of 1480 rpm, as shown in Figure 3.

Figure 3 illustrates the numerical and experimental results obtained for the pump efficiency and pressure in the presence of the centrifugal impeller. The hydraulic losses were determined through experimental tests and applied to the numerical results. At the LFR zone, the maximum efficiency difference was 5.2%, but it decreased as the flow rate increased, reaching less than 3% at DOP. The simulation trend showed a good correlation with the experimental results, which indicates the accuracy of the numerical simulations.

Several factors can cause differences in simulation results and experiments. The experimental results showed higher pressure and lower efficiency, which suggests that mechanical and volumetric losses, such as ball bearings friction, increased the pump's power consumption, leading to decreased efficiency.

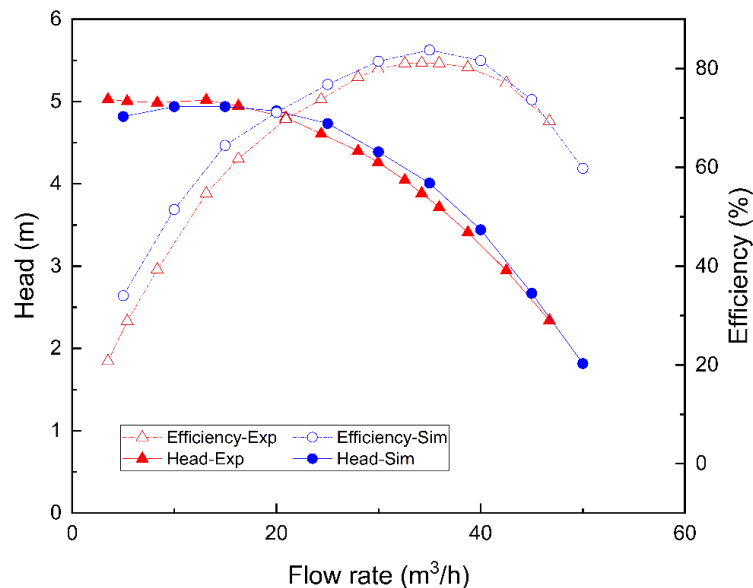


Figure 3 Experimental measurements (Exp) vs simulation results (Sim) of efficiency and head for impeller rotating at 1480 rpm

## Results and discussion

The design of the system, with the ability to separate the rotation of two rotors, offers the possibility to examine two parameters: the distance between the rotors and the direction of rotation of the inducer. The two inducers are designed to rotate in both co-rotation and counter-rotation modes, while maintaining the same geometrical characteristics and inverse tip angles. The Speed Ratio (SR) is defined as the ratio between the speed of the inducer ( $N_1$ ) and the speed of the centrifugal impeller ( $N_2$ ), where  $L$  represents the distance between the two rotors. These two parameters are identified as the study parameters. The impeller's speed is fixed at  $N_1=2960$  rpm. The curves can be classified into three zones:  $Q \leq 70$  m<sup>3</sup>/h or Low Flow Rate (LFR),  $Q = 70$  m<sup>3</sup>/h or DOP, and  $Q \geq 70$  m<sup>3</sup>/h or High Flow Rate (HFR). Table 2 presents a list of the examined parameters and their respective values.

Table 2 Different values for study parameters

Parameters	Values
Distance between the two rotors (L)	$L \leq 2$ , $L = 0.5D_{i0}$ , $L = 1D_{i0}$
Speed Ratio (SR)	Co-rotation (+1), Counter rotation (-1)

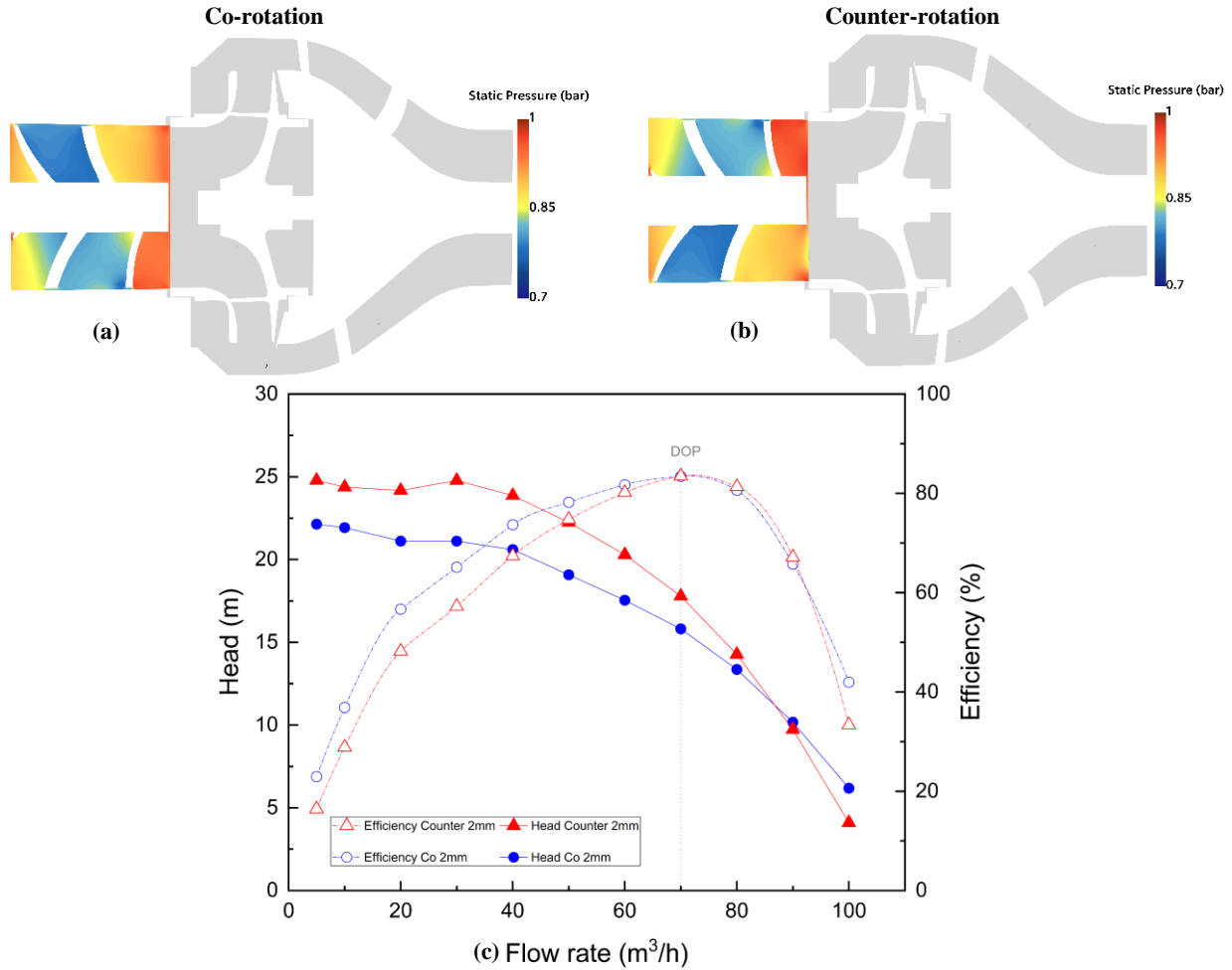


Figure 4 Efficiency and head of counter-rotating and co-rotating pumps (made of inducer and centrifugal impeller) for  $L \leq 2$  mm

Figure 4(c) displays the results for the pump efficiency and pressure in co-rotation ( $SR=1$ ) and counter-rotation ( $SR=-1$ ) modes for distances less than or equal to 2 mm ( $L \leq 2$  mm). As shown, the pump efficiency is about 8% higher in the co-rotation mode compared to the counter-rotation mode for the LFR region. However, the pump pressure is higher in the counter-rotation mode in this region, indicating that it consumes more energy than the co-rotation mode. As the flow rate increases, the slope of the increase in co-rotation efficiency decreases, resulting in both modes showing the same efficiency at DOP. However, the counter-rotation mode still generates almost 11% higher pressure than the co-rotation, demonstrating the impact of independent rotation on pump characteristics.

Figures 4(a) and 4(b) illustrate the inducer pressure distribution for co-rotation and counter-rotation modes, respectively. However, at the impeller inlet, the counter-rotation mode exhibits a pressure fluctuation, caused by a sudden change in the rotation direction. The pressure distribution within the inducer blades is identical for both modes.

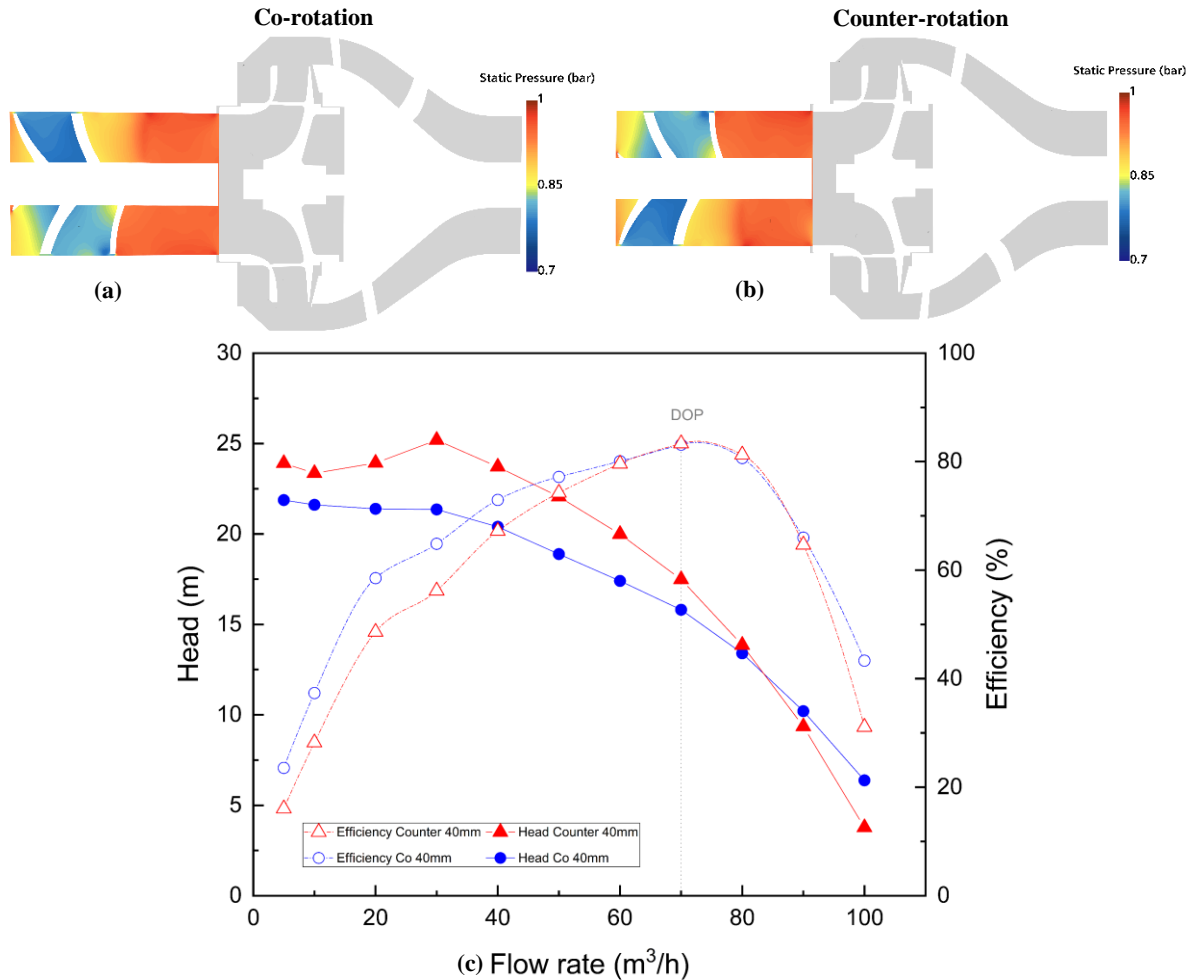


Figure 5 Efficiency and head of counter-rotating and co-rotating pumps (made of inducer and centrifugal impeller) for  $L=0.5 D_{i0}$

Figure 5 presents the simulation results for a rotor distance of 40 mm ( $L=0.5 D_{i0}$ ) between the inducer and the impeller. In Figure 5(c), it can be seen that the static pressure is higher, and the efficiency is lower for the counter-rotation mode at low flow rates. However, at the DOP, both modes have the same efficiency. The pressure distribution is identical in both rotation modes, and the pressure variations at the impeller inlet due to the minimum rotor distance are not noticeable (Figure 5(a) and 5(b)). The pump characteristics for  $L=1D_{i0}$  are shown in Figure 6. It can be concluded that changing the inducer rotation direction significantly affects pump efficiency and pressure, but rotor distance does not affect pump characteristics under non-cavitation conditions. However, rotor distance could have an impact under cavitation conditions.

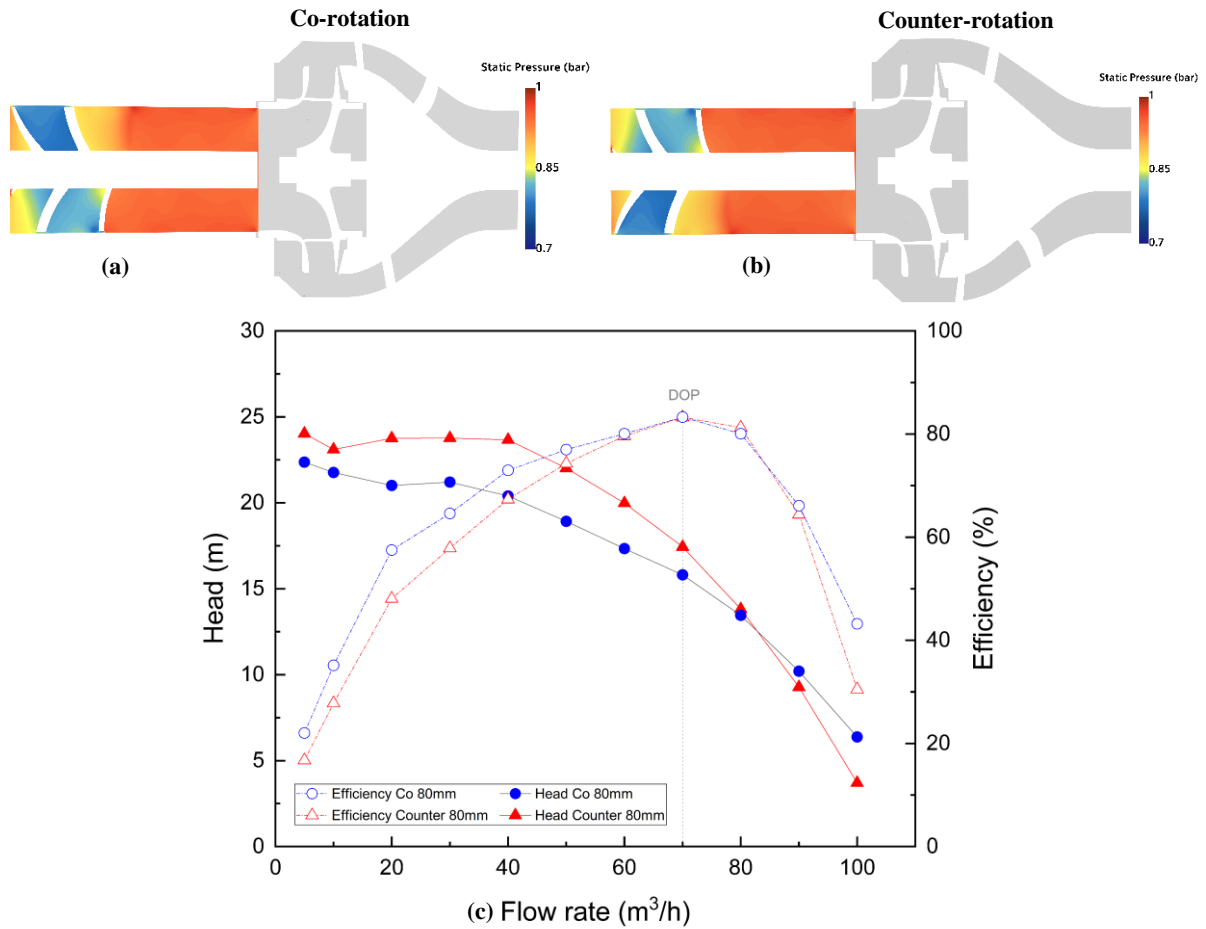


Figure 6 Efficiency and head of counter-rotating and co-rotating pump for  $L = 1D_{i0}$

Figure 7 shows the velocity triangle for the inducer and impeller in both co-rotating and counter-rotating modes. The counter-rotating inducer produces negative pre-whirl at the impeller inlet, which increases the total head of the pump according to the Euler equation.

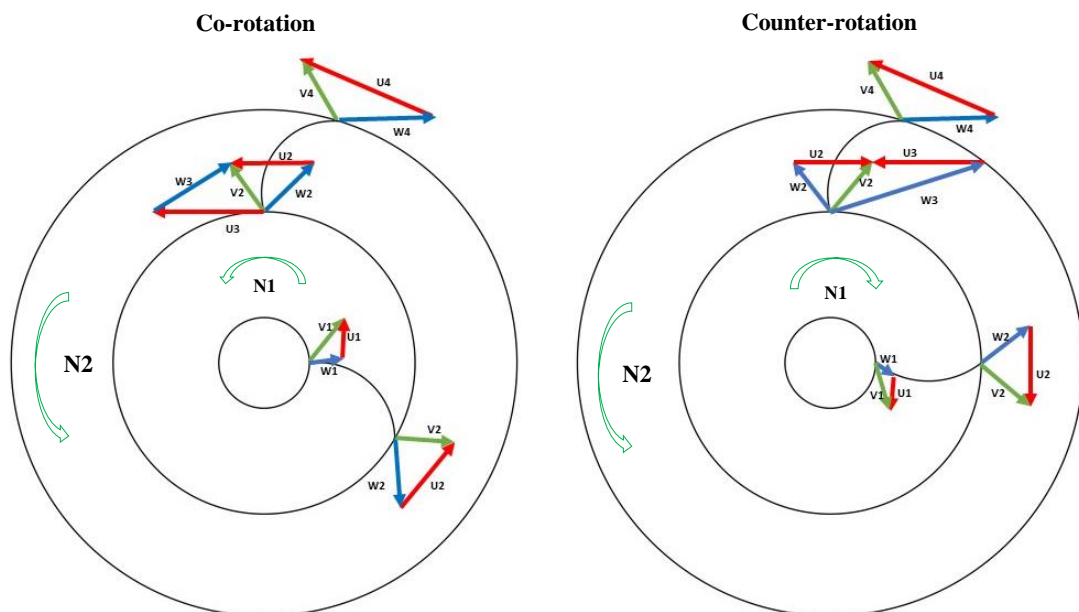


Figure 7 Velocity triangle for inducer and impeller

According to Figure 8, changing the rotational direction of the inducer can reduce the circulation between the inducer and impeller. However, the flow analysis of the pump showed that there is always some circulation between the inducer and the centrifugal impeller, which is due to the available space between the inducer and the impeller.

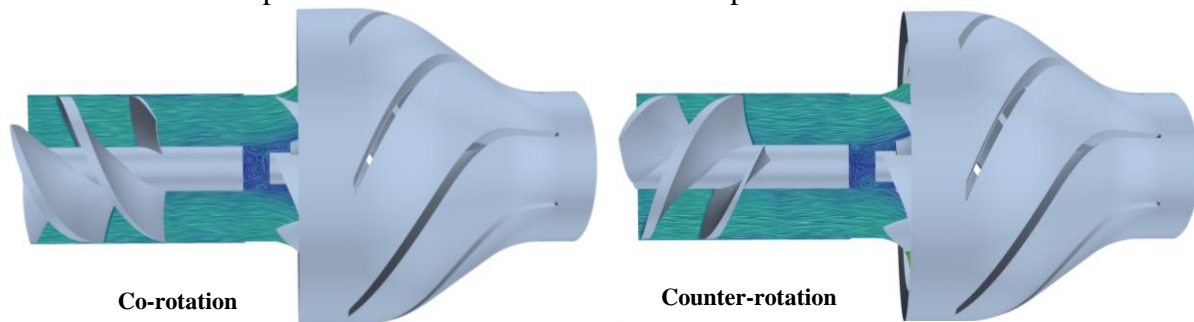


Figure 8 Flow pattern for  $L=0.5D$

## Conclusion

This paper explores the impact of an independent inducer on the centrifugal impeller in co-rotating and counter-rotating modes. The study uses simulations to analyze the head and efficiency of the pump at three different distances between the inducer and impeller. The results are grouped based on flow rate into three sections:

1. For flow rates below 70 m<sup>3</sup>/h (LFR), using counter-rotation mode can increase the pump pressure by almost 15%. However, co-rotation mode is more energy-efficient than counter-rotation mode.
2. At a flow rate of 70 m<sup>3</sup>/h (DOP), both co-rotation and counter-rotation modes have the same efficiency of 83%. However, counter-rotation mode produces 10% higher pressure than co-rotation mode. Using a counter-rotation inducer can achieve the desired pressure with less energy consumption. Furthermore, reducing the impeller rotational speed can delay cavitation.
3. For flow rates above 70 m<sup>3</sup>/h (HFR), counter-rotation mode has a negative impact on the pump characteristics, as the pump's pressure and efficiency are lower than in co-rotation mode.

In summary, this paper presents a new method to improve pump characteristics by designing the impeller and inducer separately and using two inducers with opposite angles of attack to allow for counter-rotation mode. The study investigates the effect of co-rotation and counter-rotation modes on pump characteristics and the distance between the rotors. The results show that counter-rotation mode enhances the static pressure of the pump while maintaining the same efficiency at DOP. The authors plan to conduct experimental measurements of the independent inducer and centrifugal impeller to examine the impact of changing the distance between the rotors on the pump's cavitation characteristics at the Laboratory of Fluid Engineering and Energy Systems (LIFSE) in Arts et Métiers Paris.

## References

- [1] M. Mansour, B. Wunderlich, and D. Thévenin, “Effect of tip clearance gap and inducer on the transport of two-phase air-water flows by centrifugal pumps,” *Exp. Therm. Fluid Sci.*, vol. 99, pp. 487–509, Dec. 2018, doi: 10.1016/j.expthermflusci.2018.08.018.
- [2] Z. Wei, W. Yang, and R. Xiao, “Pressure Fluctuation and Flow Characteristics in a Two-Stage Double-Suction Centrifugal Pump,” *Symmetry*, vol. 11, no. 1, p. 65, Jan. 2019, doi: 10.3390/sym11010065.
- [3] O. Coutier-Delgosha, P. Morel, R. Fortes-Patella, and JI. Reboud, “Numerical Simulation of Turbopump Inducer Cavitating Behavior,” *Int. J. Rotating Mach.*, vol. 2005, no. 2, pp. 135–142, 2005, doi: 10.1155/IJRM.2005.135.
- [4] X. Guo, Z. Zhu, B. Cui, and G. Shi, “Effects of the number of inducer blades on the anti-cavitation characteristics and external performance of a centrifugal pump,” *J. Mech. Sci. Technol.*, vol. 30, no. 7, pp. 3173–3181, Jul. 2016, doi: 10.1007/s12206-016-0510-1.
- [5] X. Guo, L. Zhu, Z. Zhu, B. Cui, and Y. Li, “Numerical and experimental investigations on the cavitation characteristics of a high-speed centrifugal pump with a splitter-blade inducer,” *J. Mech. Sci. Technol.*, vol. 29, no. 1, pp. 259–267, Jan. 2015, doi: 10.1007/s12206-014-1232-x.
- [6] T. Magne, R. Paridaens, S. Khelladi, F. Bakir, P. Tomov, and L. Pora, “Experimental Study of the Hydraulic Performances of Two Three-Bladed Inducers in Water, Water With Dissolved CO<sub>2</sub>, and Jet Fuel,” *J. Fluids Eng.*, vol. 142, no. 11, p. 111210, Nov. 2020, doi: 10.1115/1.4048143.
- [7] Z. Xu, F. Kong, H. Zhang, K. Zhang, J. Wang, and N. Qiu, “Research on Visualization of Inducer Cavitation of High-Speed Centrifugal Pump in Low Flow Conditions,” *J. Mar. Sci. Eng.*, vol. 9, no. 11, p. 1240, Nov. 2021, doi: 10.3390/jmse9111240.
- [8] R. Campos-Amezcuca, S. Khelladi, Z. Mazur-Czerwiec, F. Bakir, A. Campos-Amezcuca, and R. Rey, “Numerical and experimental study of cavitating flow through an axial inducer considering tip clearance,” p. 12.
- [9] X. Guo, Z. Zhu, G. Shi, and Y. Huang, “Effects of rotational speeds on the performance of a centrifugal pump with a variable-pitch inducer,” *J. Hydrodyn.*, vol. 29, no. 5, pp. 854–862, Oct. 2017, doi: 10.1016/S1001-6058(16)60797-7.
- [10] C. Kim, C.-H. Choi, S. Kim, and J. Baek, “Numerical study on the effects of installing an inducer on a pump in a turbopump,” *Proc. Inst. Mech. Eng. Part J. Power Energy*, vol. 235, no. 8, pp. 1877–1891, Dec. 2021, doi: 10.1177/09576509211014984.